A PROTEIN ANOMALY IN ERYTHROCYTE MEMBRANES OF PATIENTS WITH DUCHENNE MUSCULAR DYSTROPHY*

By DONALD F. H. WALLACH, SURENDRA P. VERMA, AND WILLIAM E. SINGER[‡]

From the Department of Therapeutic Radiology[‡] and Department of Neurology, Tufts-New England Medical Center, Boston, Massachusetts 02111

The muscular dystrophies constitute a group of inherited diseases with clinical patterns dominated by progressive weakness and degeneration of muscle. Duchenne muscular dystrophy (DMD)[1] is inherited in males as a recessive sex-linked characteristic. It usually appears between 3 and 7 yr of life and is characterized by progressive muscular weakness.

Available information suggests that the genetic defect of DMD produces anomalies in muscle sarcolemma and also in the plasma membranes of other cells, including erythrocytes (reviewed in reference 1). Reported erythrocyte abnormalities include irregular responses of (Na^+,K^+)-ATPase activity to ouabain (2–5), altered activities of (Ca^{++}, Mg^{++})-ATPase (6), protein kinase (4), and adenylate cyclase (7), altered cation fluxes (1), and abnormal physical properties, as detected by electron spin resonance (ESR) and fluorescence probes (8–12). While no appreciable membrane anomaly has been detected in the spectra of DMD erythrocytes with conventional ESR using 5-nitroxide stearate as probe (9), other studies with 3- and 14-nitroxide stearates (10) have revealed marked differences in the pH and temperature responses of membranes from normal vs. DMD erythrocytes. Experiments using saturation transfer ESR with 5-nitroxide stearate as a probe (11) showed significant spectral deviations in the membranes of erythrocytes from DMD patients. Fluorescence depolarization studies using perylene as a probe (12) have been interpreted as indicating a generalized lipid-related defect in DMD membranes, but lipid analyses of DMD erythrocytes do not show any consistent difference from normal (13). Some evidence for a protein defect in DMD erythrocytes has come from ESR studies using a spin-labeled maleimide probe that covalently binds to sulfhydryl groups of the anion transport protein (14).

The probe techniques used heretofore are compatible with possible abnormal lipid-protein interactions in DMD erythrocyte membranes. However, one cannot be sure whether the anomalous signals obtained from DMD erythrocytes arise from altered probe partitioning between aqueous and membrane compartments, or between membrane protein and lipid, from the reactivity of the probes with altered protein or from differential perturbation by the probe. We have therefore investigated erythrocyte membranes with Raman spectroscopy, which analyzes signals originating directly from membrane components.

Our studies on membranes from 20 DMD patients and 8 age-matched controls (15 and 5, respectively, evaluated as coded samples) provided conclusive evidence for a protein anomaly in DMD erythrocyte membranes.

Materials and Methods

Heparinized blood samples were collected from males with DMD at the time of their regular follow-up visits to the Muscular Dystrophy Association Clinic meeting at Lakeville Hospital, Lakeville, MA. At that time, functional assessments of the DMD patients were carried out and recorded according to the recommendations of Zellweger and Hanson (15). The ages of the DMD patients ranged from 4 to 14 yr, the duration of disease at the time of sampling from 0 to 8 yr, and the disease severity from Zellweger stage III to X.

Controls consisted of unaffected male siblings of the DMD patients and males who were having blood drawn as part of the initial evaluation of newly developed seizure disorders. None of the controls were taking medication at the time of blood drawing. There was no evidence of myopathy in the control population. All samples were obtained in conformity with the guidelines of the Human Investigations Review Committee, Tufts-New England Medical Center.

The diagnosis of DMD in each affected case was based on a combination of clinical features and disease course, serum creatinine kinase, and muscle biopsy. Electromyogram and nerve conduction studies were carried out in some cases.

Blood was stored on ice during transport (~45 min) before membrane isolation. Erythrocytes were washed three times with 150 mM NaCl, 5 mM phosphate (pH 7.4). The washed cells were lysed with 5 mM phosphate (pH 7.4) and erythrocyte ghosts were isolated as in reference 16. As complete Raman analyses at multiple temperatures cannot be finished on the day of blood collection, all samples were frozen in 250 mM sucrose and analyzed after thawing and further processing. Raman analyses comparing two frozen-thawed and unfrozen samples showed no effects due to freezing/thawing. All the Raman data presented are on samples thawed >15 min at 4°C and washed in 5 mM phosphate. Membranes were packed by centrifuging at 1.2×10^7 g min, at 4°C and transferred to Kimax capillaries (1.5 mm ID) for Raman spectroscopy. Raman spectra were recorded using a Ramalog (Spex Industries, Metuchen, NJ) spectrometer modified for use with an optical multichannel analyzer (OMA) (Princeton Applied Research, NJ) as in reference 17. The M6 mirror (0.85 m) of the second monochromator has been replaced by a 1 m mirror. The movable middle slit has been replaced by a 12.7 mm $\times$ 5.2 mm fixed slit and baffles milled into a aluminum block of the middle slit dimensions. The exit slit has been removed. Both 1,200-groove/mm gratings have been replaced by 600-groove/mm gratings. An additional filter has been inserted before the entrance slit to minimize Rayleigh-scattered light.

The detector, a PAR 1205D silicon-intensified target tube (SIT) (Princeton Applied Research, Princeton, NJ [PAR]) is housed in a PAR 1212 cooled housing. The PAR 1212 unit is rigidly attached to the exit port of the monochromator by an adapter adjusted to focus the Raman-scattered light onto the face of the SIT tube. The tube is precisely oriented in the optical axis. The output of the SIT is detected by a PAR 1205A optical multichannel analyzer, once the SIT tube is cooled to ~−50°, (~2 h).

To subtract background signals from sample signals, we match counts at the 0-channel: the detector output obtained with the sample in place is stored in memory A of the 1205A. The sample capillary is then displaced to a position where there is no membrane material in the beam and the Raman spectrum recorded and stored in memory B of the 1205A analyzer. The difference A − B (projected on a display scope) is plotted on an $X - Y$ recorder. The subtraction procedure results in stable base lines and reproducible Raman features. We collect 1,000 scans (32.8 ms each) per control and data point (i.e., ~50 s each). One difference data point in the transition curves takes ~2.5 min. For temperature scans we collect 1,000 scans of the CH-stretching region (2,800–3,000-cm⁻¹) per degree going from −10°C to 45°C and vice versa. Conventional scanning Raman spectroscopy was on selected samples as detailed previously (18).

Membranes from 20 patients with DMD and 8 age-matched controls were analyzed by Raman spectroscopy in the region of the tyrosine doublet. Half of these samples were analyzed

on our spectrometer in the scanning mode, and half on the Spex instrument of the Regional Spectroscopic Facility at the Massachusetts Institute of Technology, Cambridge, MA.

Results

We evaluated 20 samples without knowledge of the source of the erythrocytes. We found that on the basis of membrane thermotropic transitions and pH responses the samples could be grouped into two categories. Breaking the code after characterizing 20 samples, we found that one category corresponded to age-matched normal controls and the other to DMD patients. Membranes from the former (five samples) gave spectra and thermal transitions identical to those of normal membranes published earlier (19, 20). The 15 samples of the second group all showed abnormal thermotropic properties and all came from DMD patients. Additional uncoded comparisons (samples from five DMD patients and three age-matched controls) were confirmatory. Later studies showed clear distinctions between the spectra of membranes from DMD patients and age matched controls in the Amide I/III and tyrosine regions.

The CH-Stretching Region. We recorded OMA spectra in the carbon-hydrogen (CH)-stretching region (2,800–3,000-cm^{-1}) over the temperature range of $-30°$ to $50°C$ for all samples. The OMA spectra are comparable to those obtained by conventional recording. The CH-stretching region is marked by three prominent bands, near 2,850-cm^{-1}, 2,880-cm^{-1}, and 2,930-cm^{-1} (Fig. 1). The first two have previously been assigned to symmetric and asymmetric CH stretching (CH$_2$ methylene modes), respectively (10). The 2,930 $\pm$ 5-cm^{-1} band probably represents overlapping asymmetric CH-stretching of CH$_2$ groups and symmetric CH-stretching of CH$_3$ groups from both membrane lipids and proteins. With the exception of the 2,930-cm^{-1} feature, the CH-stretching bands in the 2,800–3,000-cm^{-1} region primarily represent the behavior of membrane lipid acyl chains.

Thermotropic Transitions. The intensity of the 2,880-cm^{-1} and 2,930 $\pm$ 5-cm^{-1} bands vary with temperature, whereas that of 2,850-cm^{-1} remains almost constant. Plots of (I_{2880}/I_{2850}) and/or (I_{2930}/I_{2850}) vs. temperature, where I represents the amplitude of a respective band, yield discontinuities (Figs. 2 and 3), which correspond to the thermal transitions of membrane lipid or lipid/protein phases (18). Plots of [I_{2880}/I_{2850}] vs. temperature for erythrocyte membranes obtained by OMA-Raman and conventional Raman spectroscopy give identical values for transition temperatures. However, slight differences occur in the numerical values of the ratio [I_{2880}/I_{2850}]; these may be attributed to the distribution of bands and background in various OMA channels. We calculate the intensity ratio of CH-stretching bands using the base line joining the intensity minima in that region of the spectrum. These minima generally lie at 2,820 $\pm$ 5 cm^{-1} and 3,000 $\pm$ 5 cm^{-1}.

Fig. 2A shows the variation of [I_{2880}/I_{2850}] vs. temperature for membranes from normal patients. The curve shows two transitions. The first is relatively small, sharp, and symmetrical, starting around 13°C and ending around 21°C (midpoint 15.6°C, Table I). This transition probably represents protein-associated lipids, as liposomes made from isolated membrane lipids show no transition in this temperature range. The second transition starts around $-12°C$ and ends near 2°C. Since it occurs in lipid extracted from membranes, this transition probably represents unencumbered lipid. The temperatures of the two transitions are identical to those of numerous samples from normal adults (19).

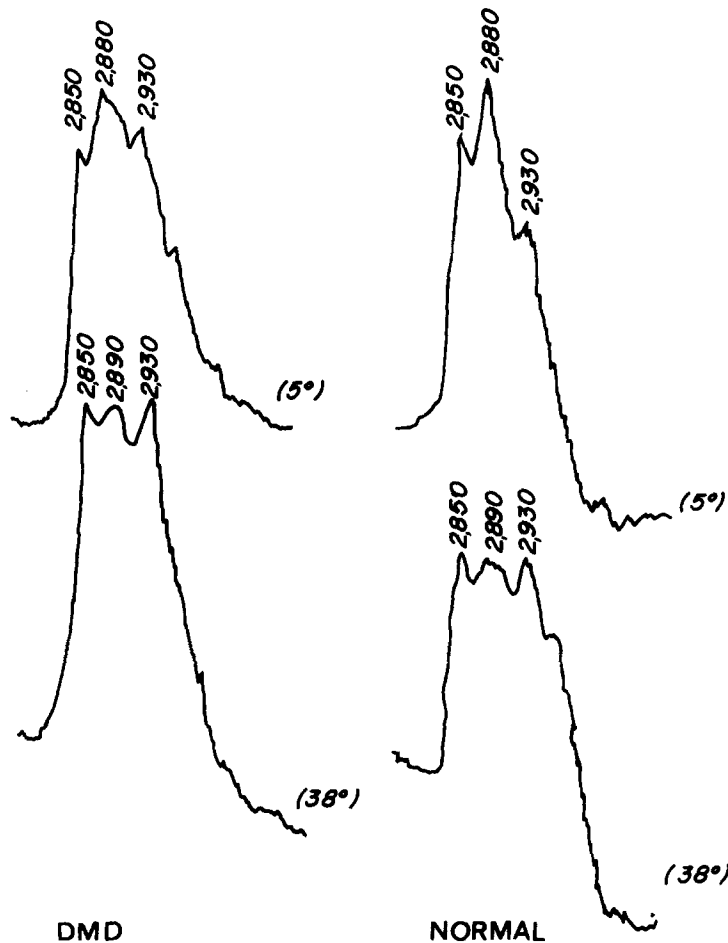DMD   NORMAL

Fig. 1.   Raman spectra in the CH-stretching region of normal and DMD erythrocytes at marked temperatures (pH 7.4; phosphate buffer). Spectra were recorded by OMA. Laser power at the sample 300 mW. The total recording time for one spectrum is (50 s).

Fig. 2 B shows the high temperature transition reported by the plot of $[I_{2930}/I_{2850}]$ vs. temperature for normal erythrocyte ghosts at pH 7.4. $[I_{2930}/I_{2850}]$ changes very little below 32°C. At slightly higher temperatures, the ratio increases sharply and levels off at about 42°C. This thermotropism is identical to that reported by us for erythrocytes from normal adults (20) and for plasma membranes from normal lymphoid cells (21).

The plot of $[I_{2880}/I_{2850}]$ vs. temperature for membranes from DMD patients is shown in Fig. 3 A. $[I_{2880}/I_{2850}]$ is constant between 7° and 45°C. The 13°C/21°C discontinuity of membranes from normal individuals is missing. All but two of the coded DMD samples showed a broad transition between −15°C and 7°C. In the remaining two cases, this transition extended between −20°C and 1°C.

The intensity of the 2,930 ± 5 cm^{-1} band in DMD ghosts (pH 7.4) changes very little up to 36°C in contrast to normal ghosts which show a marked increase of $[I_{2930}/I_{2850}]$ above 32°C. Above 35°C it rises gradually and continues to increase even above
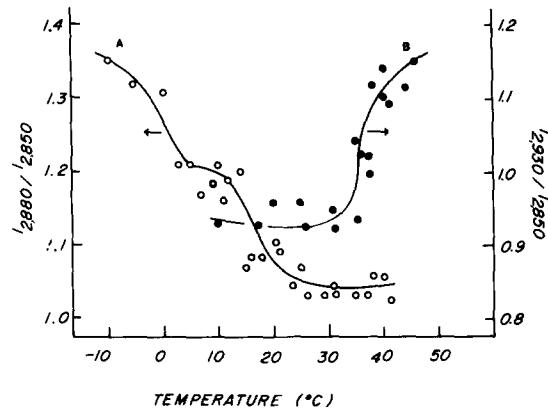
FIG. 2. (A) Variation of $[I_{2880}/I_{2850}]$ vs temperature for normal membranes (pH 7.4) (left ordinate) (O). (B) Variation of $[I_{2930}/I_{2850}]$ vs temperature for normal erythrocyte ghosts (pH 7.4) (right ordinate) (●).
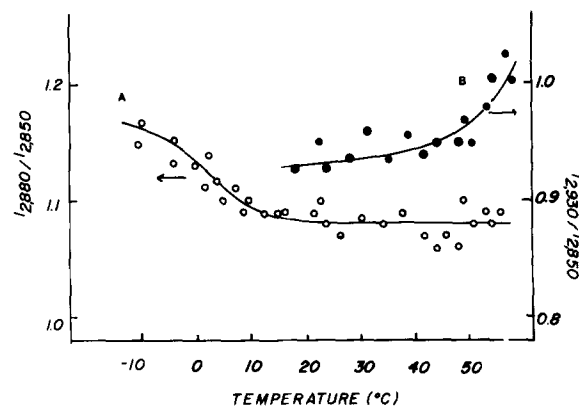

FIG. 3. (A) Variation of $[I_{2880}/I_{2850}]$ vs temperature for DMD erythrocyte ghosts (pH 7.4) (left ordinate) (O). (B) Variation of $[I_{2930}/I_{2850}]$ vs temperature for DMD erythrocyte ghosts (pH 7.4) (right ordinate) (●).

TABLE I

CH-Stretching Raman Parameters for Normal and DMD Membranes and Thermal Transition
Temperatures (T_c) as Calculated from Plots of $[I_{2880}/I_{2850}]$ and $[I_{2930}/I_{2850}]$ vs. Temperature

Sample	Average ratio change*		T_c (midpoint)	
	$[I_{2880}/I_{2850}]$	$[I_{2930}/I_{2850}]$	$[I_{2880}/I_{2850}]$	$[I_{2930}/I_{2850}]$
Normal (n = 8)	1.05 to 1.20 (40°–+10°)	0.92 to 1.15 (30°–+50°)	15.6	39° (pH 7.4)
	1.20 to 1.35 (10°––10°)		—	30° (pH 6.5)
			—	7° (pH 5.7)
DMD (n = 20)	1.09 to 1.15 (40°––10°)	0.9 to 1.12 (30°–+50°)	3°	45° (pH 7.4)
			—	24° (pH 5.7)
			$P < 0.001$	

* These values are ~20–25% less than those obtained by scanning Raman spectroscopy (18).
‡ Calculated for n = 8 (normal/DMD), using Student's t test.

50°C, whereas in normal membranes it levels off at 42°C. A representative plot of $[I_{2930}/I_{2850}]$ vs. temperature is shown in Fig. 3 B.

pH Response.

The intensity of the 2,930 ± 5-cm^{-1} band of normal membranes increases steadily as pH is reduced from 7.4 ($[I_{2930}/I_{2850}]$ = ~0.9) to pH 6.0 ($[I_{2930}/I_{2850}]$ = ~1.15) at 21°C. This pH response is identical to that observed by us (19) with ghosts from normal adults where the transition midpoint of $[I_{2930}/I_{2850}]$ shifts from about 40°C at pH 7.4 to about 30°C at pH 6.5. The absolute values of $[I_{2930}/I_{2850}]$ are ~20% higher when measured by conventional scanning Raman spectroscopy, but the positions of the temperature curves are identical. Representative plots of $[I_{2930}/I_{2850}]$ vs. temperature at various pH values are shown in Fig. 4 A. In membranes from DMD patients, in contrast to normals, $[I_{2930}/I_{2850}]$ does not change appreciably between pH 7.4 and pH 6.0 (~0.95) at 21°C.

At pH 5.7, $[I_{2930}/I_{2850}]$ from DMD membranes indicates a thermal transition that starts around 12°C and does not seem to be complete until about 42°C (Fig. 4 B). As the pH is further lowered to 5.3, the transition disappears (Fig. 4 C). The maximum value for $[I_{2930}/I_{2850}]$ remains constant, within experimental error (10%), between 2°C to 45°C.

Amide I and Amide III Region.

The band positions in the Amide I (1,600–1,700-cm^{-1}) regions vary with the secondary structure of membrane proteins (18). In membranes from normal subjects, the Amide I region shows a band at 1,660 ± 5-cm^{-1} (assigned to α- and disordered configuration) which shifts to 1,635 ± 5 cm^{-1} when membranes are suspended in D_2O (Fig. 5). The Amide III region (1,200–1,300-cm^{-1}) gives a broad band at 1,270 ± 5 cm^{-1} (assigned to α- and disordered configurations). DMD membrane samples give
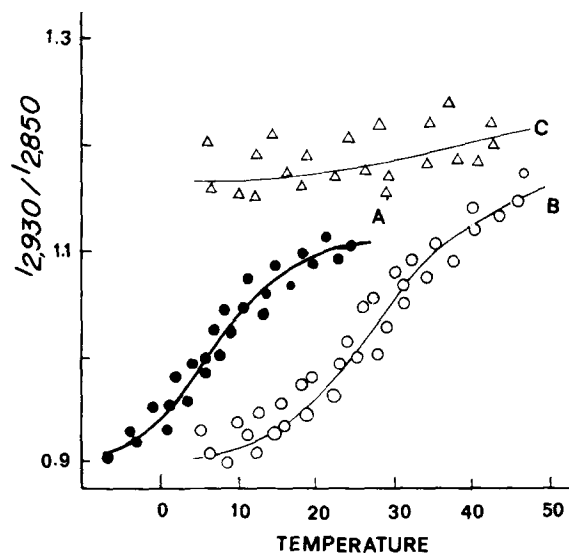

FIG. 4. Variation of $[I_{2930}/I_{2850}]$ vs temperature at various pHs for normal and DMD erythrocyte ghosts. (A) Normal membranes at pH 5.7; (●). (B) DMD membranes at pH 5.7; (O). (C) DMD membranes at pH 5.3; (△).
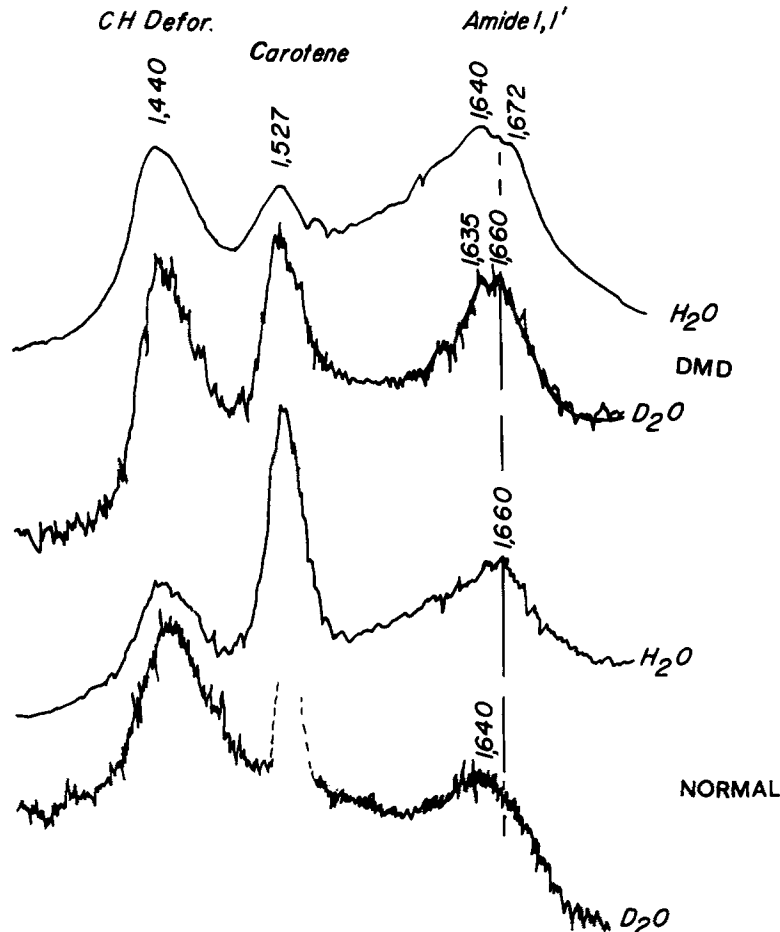
FIG. 5. Raman spectra in the 1400–1700-cm^{-1} region of normal and DMD membranes suspended in H$_2$O/D$_2$O buffers (pH 7.4 phosphate buffer). The recording conditions are the same as in Fig. 1.

the same strong band at 1,660 ± 5-cm^{-1}, as normals, but also show a band at 1,640-cm^{-1} and a shoulder around 1,672 ± 3-cm^{-1} (Fig. 5); these features indicate the presence of β-configuration. The 1,660 ± 5-cm^{-1} band of DMD membranes does not disappear upon taking the samples up in D$_2$O while in normal membranes it shifts to about 1,635 cm^{-1} (Fig. 5, compare H$_2$O and D$_2$O spectra for DMD membranes). This suggests that this band arises from cis C=C bonds predominantly. That DMD membranes has some β-structured proteins is also indicated by the presence of a band at 1,235 ± 5-cm^{-1} (Fig. 6), lacking in erythrocyte ghosts from age-matched controls.

The Tyrosine Doublet.

Well-resolved spectra were obtained in the 700–900-cm^{-1} region from both DMD and control membranes at pH 7.4. The two components of the tyrosine doublet lie at 855 and 830 cm^{-1}. The 855-cm^{-1} band of DMD membranes is substantially more prominent than in controls (Fig. 7). The ratio [I_{855}/I_{830}] ranges from 0.7 to 0.8 in 20 DMD samples, compared with 0.5 to 0.6 in 8 control samples. The difference between the DMD and control samples, calculated by the t test is highly significant ($P <$
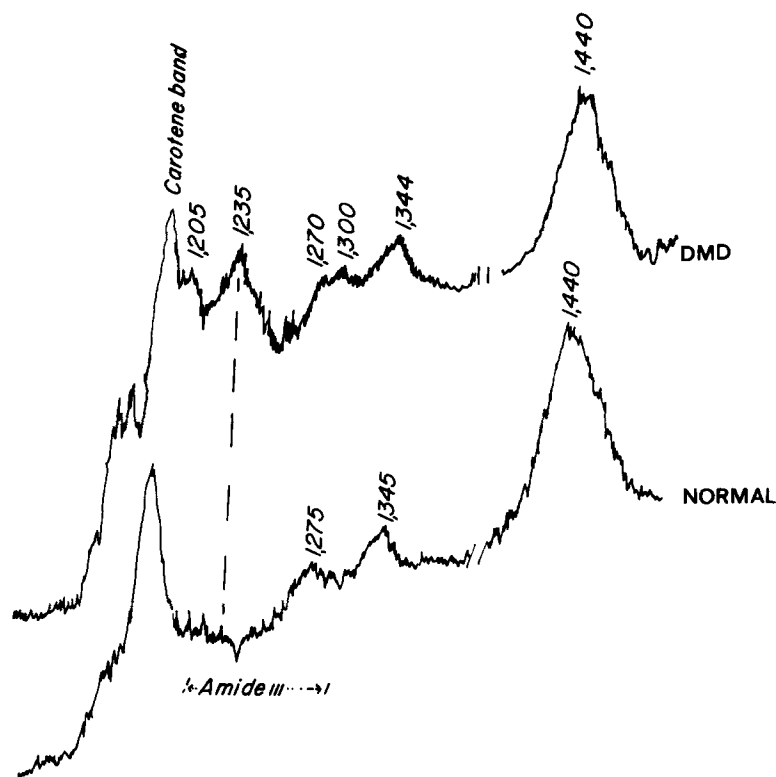
Fig. 6.   Raman spectra in the 1,200–1,500-cm^{-1} region of normal and DMD membranes at pH 7.4 (phosphate buffer). The recording conditions are the same as in Fig. 1.

0.001). The ratio difference suggests a greater exposure of tyrosine residues in DMD membranes to a polar environment (22).

Discussion

When a substance is irradiated with monochromatic light such as provided by an optical laser, most of the light is transmitted, some of it is scattered at the frequency of the incident light (Rayleigh scattering) and traces are scattered at lower and higher frequencies (Raman scattering). The difference in the frequency between the incident light and a Raman-scattered line corresponds to the frequency of vibration, in reciprocal centimeters, of the bond giving rise to the scattered light.

The band near 2,880-cm^{-1} in the Raman spectra of erythrocyte ghosts arises from asymmetric CH-stretching of methylenes in fatty acyl chains (18, 19). The intensity of this band, relative to that of the thermally stable band at 2,850-cm^{-1}, i.e. [I_{2880}/I_{2850}], is known to decrease with the transition from the crystalline (gel) to the liquid state of phospholipids (18). The intensity changes (and frequency shifts) observed with such transitions involve altered Fermi resonance interactions between methylene deformation modes and symmetric methylenic CH-stretching modes and reflect changes in the interchain interaction of adjacent lipid molecules (23, 24).

We have previously shown that the plots [I_{2880}/I_{2850}] vs. temperature show inflections

at the transition temperatures of lipid and lipid-protein phases in erythrocyte ghosts from normal adults (19) and plasma membranes of a variety of lymphoid cells (18, 21). The thermal transition below 0°C, as determined by these plots, probably represent phospholipids containing unsaturated acyl chains. However, transitions may shift to higher temperatures when unsaturated lipids are mixed with saturated lipids or certain proteins (25). We postulate that the thermotropic transition in $[I_{2880}/I_{2850}]$ with onset/completion temperatures of $-12°C/2°C$ and $13°C/21°C$, represent lipid and lipid/protein phases, respectively, as the latter does not occur in liposomes made from extracted membrane lipids (18). That the $13°C/21°C$ transition is absent or diffuse in DMD membranes suggests lesser *protein* interaction with lipid, especially since careful comparisons of lipids from DMD and normal erythrocyte membranes show no significant differences (13).

The changes in $[I_{2930}/I_{2850}]$ represent shifts in the positions of amino acid methyl residues that occur with protein folding/unfolding analogous to the process that occurs at much higher temperatures with soluble proteins (26). A related response also occurs with changes of membrane potential (27). The large bulk of erythrocyte membrane protein does not exhibit any thermotropic change in state until above 48°C (28).

In the case of normal membranes plots of $[I_{2930}/I_{2850}]$ vs. temperature reveal a change of protein state with onset/completion temperatures of $33°C/42°C$ (midpoint 39°C) and recent independent data (29) on membranes from normal individuals indicate that the principal protein contributing to the 39°C thermotropism is the anion transport protein (30). In DMD membranes this transition occurs at substantially higher temperatures (onset near 36°C, midpoint 45°C), as if a smaller proportion of protein were lipid-associated.

As with most soluble proteins, reduction of pH lowers the temperature at which unfolding occurs. However, a change from pH 7.4 to 6.0 lowers the unfolding temperature of erythrocyte membrane protein by more than 10°C (26), while a similar reduction in the unfolding temperature of soluble proteins requires a shift to pH 2-3. The lower thermal susceptibility of DMD proteins upon pH reduction suggests a lesser interaction with membrane lipid.

Conformational analyses are also compatible with reduced protein/lipid interactions in DMD membranes. A number of considerations (reviewed in reference 31) indicate that protein segments penetrating membranes are in α- or 3_{10}-helical conformation, and that β-structures or unordered conformations are not compatible with insertion into an apolar membrane domain. The fact that both Amide I and Amide III spectra indicate significant proportions of β-structure in DMD but not in normal membranes therefore suggests that a greater proportion of protein is not intimately associated with lipid in DMD erythrocyte membranes.

The tyrosine spectra lead to similar conclusions. They suggest greater exposure of tyrosine residues in DMD membrane protein to a polar environment that is compatible with reduced protein-lipid interaction.

The anomalies in DMD membranes observed by Raman spectroscopy are very prominent. One must therefore enquire about the source of the Raman signals. As the intensity of Raman scattering depends on the mass of scattering material in the laser beam, whatever component is responsible for the unique properties of DMD membranes must comprise a large proportion of integral membrane protein. At the same

time, the 15.6°C transition in $[I_{2880}/I_{2850}]$ does not represent all of the membrane lipid, but as noted above, a small fraction normally associated with protein (19). Likewise, the normal 39°C transition in $[I_{2930}/I_{2850}]$ does not represent all membrane protein, only the small proportion that is lipid-associated protein within the membrane core (20) and responsive to membrane potential (27). The Amide I/Amide III and tyrosine differences between DMD and normal membranes similarly represent only a portion of membrane protein.

What component of membrane protein might account for the anomalies in DMD membranes? The most prominent protein in erythrocyte membranes including DMD membranes, is the anion transport protein (30). This protein accounts for at least 25% of the total protein mass of erythrocyte membranes (16, 32) and an even greater proportion of peptide associated with the apolar membrane core. Each erythrocyte contains ~1.2 1× 10^6 molecules of anion transport protein (32), normally arranged as 0.6 × 10^6 dimers, corresponding to the number of hydrophilic channels through the erythrocyte surface (37). Each anion-transport protein molecule has an M_r 15,000–17,000 segment and at least an additional M_r 9,000–10,000 portion intimately associated with the membrane core (33–36). In contrast, the transmembrane segment of glycophorin (~4 × 10^6 copies per cell) has an M_r of only ~3,000 (31) and those of band 4.2–4.5 (0.2 × 10^6 copies per cell) probably <9,000. Other membrane-penetrating proteins, such as Na^+,K^+-ATPase and Mg^{2+}, Ca^{2+}-ATPase are much less prevalent in the membrane (10^3–10^4 cell; reference 32). According to this information, the anion-transport protein accounts for >90% of the peptide associated with the core of erythrocyte membranes and must therefore contribute in a major way to the protein Raman signals from erythrocyte membranes. For this reason alone, it will be necessary to evaluate the properties of anion transport protein in DMD membranes. Also, other data on DMD are not incompatible with a possible erythrocyte anion transport protein defect. ESR studies with nitroxide stearate spin probes (10), demonstrating loss of the 15.6°C transition, and also of normal pH response in DMD membranes are directly comparable to our results. Abnormal signals reported after the labeling of DMD membranes with an N-methylmaleimide spin probe (14) reacting primarily with thiols of the anion transport protein also suggest that this protein may be anomalous in DMD. Finally, freeze fracture electron microscopy reveals an abnormally low number of intramembranous particles in DMD membranes (37). These particles primarily represent the transmembrane segments of the anion transport protein (32).

Since the pathway of anion transport protein peptide through the erythrocyte membrane has been mapped (33–36) one can directly test whether this protein is defective in DMD and possibly incorrectly inserted into the plasma membrane.

Summary

Raman spectroscopic comparisons of erythrocyte membranes from 20 patients with Duchenne muscular dystrophy and 8 age-matched controls indicate a prominent and consistent protein anomaly in the patient samples. This was apparent in the following: (a) CH-stretching signals from control membranes reveal a thermotropic transition at 15.6°C, attributable to a protein/lipid phase that is lacking in dystrophic membranes. (b) CH-stretching signals from control membranes also show a protein transition at 39°C [pH 7.4] that is shifted to 45° in dystrophic membranes. (c) A reduction in pH

to 5.7 shifts this transition from 39°C to 7°C in normal membranes and from 45°C to 24°C in dystrophic membranes. (d) The Amide I/Amide III regions indicate a significant proportion of β-structured peptide in dystrophic but not normal membranes. (e) Analysis of tyrosine signals indicates greater polar exposure of tyrosine hydroxyl groups in dystrophic vs normal membranes. All of the differences between dystrophic and normal membranes are highly significant ($P < 0.001$).

References

1. Plishker, G. A., and S. H. Appel. 1980. Red blood cell alterations in muscular dystrophy: the role of lipids. *Muscle & Nerve.* **3:**70.
2. Brown, H. D., S. K. Chattopadhyay, and A. B. Patel. 1967. Erythrocyte abnormality in human myopathy. *Science (Wash. DC).* **157:**1577.
3. Dunn, M. J., A. H. M. Burghes, and V. Dubowitz. 1980. Erythrocyte ghost Na^+,K^+-adenosine triphosphatase in Duchenne muscular dystrophy. *J. Neurol. Sci.* **46:**209.
4. Peter, J. B., M. Worstold, and C. M. Pearson. 1969. Erythrocyte ghost adenosine triphosphatase (ATPase) in Duchenne dystrophy. *J. Lab. Clin. Med.* **74:**103.
5. Siddiqui, P. Q., and R. J. Pennington. 1977. Effect of ouabain upon erythrocyte membrane adenosine triphosphatase in Duchenne muscular dystrophy. *J. Neurol. Sci.* **34:**365.
6. Luthra, M. G., E. Z. Stern, and H. D. Kim. 1979. $(Ca^{2+} + Mg^{2+})$-ATPase of red cells in Duchenne and myotonic dystrophy: effect of soluble extoplasmic activator. *Neurology.* **29:**835.
7. Mawatari, S., M. Schonberg, and M. Olarte. 1976. Biochemical abnormalities of erythrocyte membranes in Duchenne dystrophy. Adenosine triphosphatase and adenyl cyclase. *Arch. Neurol.* **33:**489.
8. Barchi, R. L. 1980. Physical probes of biological membranes in studies of the muscular dystrophies. *Muscle & Nerve.* **3:**82.
9. Butterfield, D. A., D. B. Chestnut, S. H. Appel, and A. D. Roses. 1976. Spin label study of erythrocyte membrane fluidity in myotonic and Duchenne muscular dystrophy and congenital myotonia. *Nature (Lond.)* **264:**169.
10. Sato, B., K. Nishikida, I. Samuels, and F. Tyler. 1978. Electron spin resonance studies of erythrocytes from patients with Duchenne muscular dystrophy. *J. Clin. Invest.* **61:**251.
11. Wilkerson, L. S., R. C. Perkins, Jr., R. Roelofs, L. Swift, I. R. Dalton, and J. H. Park. 1978. Erythrocyte membrane abnormalities in Duchenne muscular dystrophy monitored by saturation transfer electron paramagnetic resonance spectroscopy. *Proc. Natl. Acad. Sci. USA.* **75:**838.
12. Sha'afi, R. I., S. B. Rodan, R. L. Hintz, S. M. Fernandez, and G. A. Rodan. 1975. Abnormalities in membrane microviscosity and ion transport in genetic muscular dystrophy. *Nature (Lond.)* **254:**525.
13. Koski, C. L., F. B. Jungalwala, and F. H. Kolodny. 1978. Normality of erythrocyte phospholipids in Duchenne muscular dystrophy. *Clin. Chem. Acta.* **85:**295.
14. Butterfield, D. A. 1977. Electron spin resonance investigations of membrane proteins in muscle diseases. *Biochim. Biophys. Acta.* **470:**1.
15. Zellweger, H., and J. W. Hanson. 1968. Psychomatic studies in muscular dystrophy, type 3 (Duchenne) in Developmental Medicine and Child Neurology. Vol. 9. pp. 576–581.
16. Fairbanks, G., T. L. Steck, and D. F. H. Wallach. 1971. Electrophoretic analysis of the major polypeptides of human erythrocyte membranes. *Biochemistry.* **10:**2606.
17. Verma, S. P., and D. F. H. Wallach. 1982. Action of ionizing radiation on lipid-protein interaction. *Biochem. Biophys. Res. Commun.* **105:**105.

18. Wallach, D. F. H., S. P. Verma, and J. F. Fookson. 1979. Application of laser Raman spectroscopy to the analysis of membrane structure. *Biochim. Biophys. Acta.* **559:**153.

19. Verma, S. P., and D. F. H. Wallach. 1976. Multiple thermotropic state transitions in erythrocyte membranes: a laser Raman study of CH stretching vibrations and acoustical modes. *Biochim. Biophys. Acta.* **436:**307.

20. Verma, S. P., and D. F. H. Wallach. 1976. Erythrocyte membranes undergo cooperative, pH sensitive state transitions in the physiological temperature range: evidence from Raman spectroscopy. *Proc. Natl. Acad. Sci. USA.* **73:**3558.

21. Verma, S. P., R. Schmidt-Ullrich, W. S. Thompson, and D. F. H. Wallach. 1977. Differences between the structural dynamics of plasma membranes of normal hamster lymphocytes and lymphoid cells neoplastically transformed by Simian virus 40 as revealed by laser Raman spectroscopy. *Cancer Res.* **37:**3490.

22. Chen, M. C., and R. C. Lord. 1976. Laser Raman spectroscopy of the thermal unfolding of ribonuclease. *Biochemistry.* **15:**1889.

23. Snyder, R. G., S. L. Hsu, and G. Krimm. 1978. Vibration spectra in the CH stretching region and the structure of the polymethylene chain. *Spectrochim. Acta Part A Mol. Spectrosc.* **34:**395.

24. Gaber, B., and W. L. Peticolas. 1977. On the quantitative interpretation of biomembrane structure by Raman spectroscopy. *Biochim. Biophys. Acta.* **465:**260.

25. Verma, S. P., D. F. H. Wallach, and J. D. Sakura. 1980. Raman analysis of the thermotropic behavior of lecithin-fatty acid systems and their interaction with proteolipid apoprotein. *Biochemistry.* **19:**574.

26. Verma, S. P., and D. F. H. Wallach. 1977. Changes of Raman scattering in the CH-stretching during thermally-induced unfolding of ribonuclease. *Biochem. Biophys. Res. Commun.* **74:**473.

27. Mikkelsen, R. B., S. P. Verma, and D. F. H. Wallach. 1978. Effect of transmembrane ion gradients on Raman spectra of sealed, hemoglobin-free erythrocyte membrane vesicles. *Proc. Natl. Acad. Sci. USA.* **75:**5478.

28. Lysko, K. A., R. Carlson, R. Taverna, J. Snow, and J. F. Brandts. 1981. Protein involvement in structural transition of erythrocyte ghosts. Use of thermal gel analysis to detect protein aggregation. *Biochemistry.* **20:**5570.

29. Nigg, E. A., and R. J. Cherry. 1979. Influence of temperature and cholesterol on the rotational diffusion of Band 3 in human erythrocyte membrane. *Biochemistry.* **18:**3457.

30. Cabantchik, Z. J., P. A. Knauf, and A. Rothstein. 1978. The anion transport system of the red blood cell. The role of membrane protein evaluated by the use of probes. *Biochem. Biophys. Acta.* **515:**239.

31. Engelman, D. M., and Steitz, T. A. 1981. The spontaneous insertion of proteins into and across membranes. The helical hairpin hypothesis. *Cell.* **23:**411.

32. Morrison, M. 1981. Protein architecture of the erythrocyte membrane *In* The Function of Red Blood Cells: Erythrocyte Pathobiology. D. F. H. Wallach, editor. A. R. Liss, Inc., New York. pp. 17–34.

33. Rothstein, A., M. Ramjesingh, S. Grinstein, and P. A. Kinauf. 1980. Protein structure in relation to anion transport in red cells. *Ann. N. Y. Acad. Sci.* **341:**433.

34. Drickamer, L. K. 1977. Fragmentation of band 3 polypeptide from human erythrocyte membranes. *J. Biol. Chem.* **252:**6909.

35. Williams, D. G., R. E. Jenkins, and M. J. A. Tanner. 1979. Structure of the anion-transport protein of the human erythrocyte membrane. *Biochem. J.* **181:**477.

36. Kempf, C., C. Brock, H. Sigrist, M. J. A. Tanner, and P. Zahler. 1981. Interaction of phenylisothiocyanate with human erythrocyte band 3 protein. *Biochim. Biophys. Acta.* **641:**88.

37. Schotland, D. L., E. Bonilla, and Y. Wakagama. 1980. Application of the freeze fracture technique to the study of human neuromuscular disease. *Muscle & Nerve.* **3:**21.